

Evaluation of free energy landscapes from manipulation experiments

A. Imparato and L. Peliti

Dipartimento di Scienze Fisiche and INFN-Sezione di Napoli, Università “Federico II”
Complesso Universitario di Monte S. Angelo, I-80127 Napoli (Italy)

E-mail: imparato@na.infn.it, peliti@na.infn.it

Abstract. A fluctuation relation, which is an extended form of the Jarzynski equality, is introduced and discussed. We show how to apply this relation in order to evaluate the free energy landscape of simple systems. These systems are manipulated by varying the external field coupled with a systems’ internal characteristic variable. Two different manipulation protocols are here considered: in the first case the external field is a linear function of time, in the second case it is a periodic function of time. While for simple mean field systems both the linear protocol and the oscillatory protocol provide a reliable estimate of the free energy landscape, for a simple model of homopolymer the oscillatory protocol turns out to be not reliable for this purpose. We then discuss the possibility of application of the method here presented to evaluate the free energy landscape of real systems, and the practical limitations that one can face in the realization of an experimental set-up.

Keywords: Fluctuations (Theory) , Energy landscapes (Theory), Mechanical properties (DNA, RNA, membranes, bio-polymers) (Theory)

1. Introduction

In the recent years, a number of manipulation experiments have been performed with the aim of gathering information on the equilibrium properties of complex molecular systems, such as biopolymers [1]. In particular, in a class of these experiments the Jarzynski equality (JE) [2, 3, 4, 5] has been exploited in order to evaluate the equilibrium free energy landscape of the system, even if the system is no more at equilibrium during the manipulation experiment.

In the present work, we wish to investigate under what conditions the use of the JE in its several forms is effective for the evaluation of the free energy landscape of a small system. Indeed, the JE requires the evaluation of the average of $\exp(-\beta W)$, where $\beta = 1/k_B T$ (T is the temperature) and W is the work exerted on the system. This quantity has a wide distribution, even if the distribution of W is comparatively narrow, and it is not clear *a priori* when sufficient statistics for its evaluation can be mustered [6]. Typically one wishes to evaluate the free energy landscape of the system as a function of a collective coordinate M which accessibly represents a semimacroscopic state of the system. For example, in the case of pulling experiments, one takes for M the elongation of the molecule. One thus needs to introduce extended forms of the JE in order to evaluate the detailed free energy landscape as a function of the internal characteristic variable. By combining the JE and the histogram method (cfr. [7, 8, 9, 10]) one is able to evaluate the free energy of a constrained equilibrium state in which the collective coordinate assumes a fixed value.

The article is organized as follows. In section 2, we derive the extended form of the JE, which connects the work done on a manipulated system to its free energy landscape. In section 3 we review the histogram method and show how it can be exploited to evaluate free energy landscapes of manipulated systems. We then apply the histogram method to evaluate the free energy landscape of a mean field Ising model, section 4, and of a simple model of homopolymer, section 5. We discuss our results and conclude in section 6.

2. The basic identity

We shall now briefly recall the derivation of the basic identity of the histogram method.

Let us consider a system described by the hamiltonian $\mathcal{H}_0(x)$, where x identifies its microscopic state. Let us also assume that the system is originally at equilibrium, so that its distribution in phase space is described by the canonical distribution function

$$\rho_0(x) = \frac{e^{-\beta \mathcal{H}_0(x)}}{Z_0}, \quad (1)$$

where

$$Z_0 = \int dx e^{-\beta \mathcal{H}_0(x)} \quad (2)$$

is the corresponding partition function. We shall assume that the system is manipulated in the following way. Let $M(x)$ be an observable quantity (a sufficiently smooth function of the microscopic state of the system) and $U_\mu(M)$ a function of M , dependent on a parameter μ . In the initial state, without loss of generality, we take $\mu = 0$ and $U_0(M) \equiv 0$. The manipulation

protocol is defined by assigning a function $\mu(t)$, ($0 \leq t \leq t_f$), where $\mu(0) = 0$ and $\mu(t_f) = \mu$. The time-dependent hamiltonian of the manipulated system is $\mathcal{H}_{\mu(t)}(x, t) = \mathcal{H}_0(x) + U_{\mu(t)}(M(x))$. The work exerted on the system up to time t is a random quantity which depends on the trajectory $x(t)$ that the system follows in phase space:

$$W = \int_0^t dt' \dot{\mu}(t') \left. \frac{\partial U_{\mu}(M(x(t'))) }{\partial \mu} \right|_{\mu=\mu(t')}. \quad (3)$$

The joint probability distribution $\Phi(x, W, t)$ of the microscopic state x and the accumulated work W satisfies the partial differential equation [9, 11, 12, 13]

$$\frac{\partial \Phi}{\partial t} = \mathcal{L}_{\mu(t)} \Phi - \dot{\mu}(t) \frac{\partial U_{\mu(t)}(M(x))}{\partial \mu} \frac{\partial \Phi}{\partial W}. \quad (4)$$

Here, \mathcal{L}_{μ} is an evolution operator whose equilibrium distribution, for any μ , is the canonical distribution defined by the hamiltonian $\mathcal{H}_{\mu}(x) = \mathcal{H}_0(x) + U_{\mu}(M(x))$:

$$\mathcal{L}_{\mu} \frac{e^{-\beta \mathcal{H}_{\mu}(x)}}{Z_{\mu}} = 0, \quad (5)$$

where, of course, $Z_{\mu} = \int dx e^{-\beta \mathcal{H}_{\mu}(x)}$. Let us now define the generating function $\Psi(x, \lambda, t)$ of the distribution of W via the equation

$$\Psi(x, \lambda, t) = \int dW e^{\lambda W} \Phi(x, W, t). \quad (6)$$

Then $\Psi(x, \lambda, t)$ satisfies the differential equation

$$\frac{\partial \Psi}{\partial t} = \mathcal{L}_{\mu(t)} \Psi + \lambda \dot{\mu}(t) \frac{\partial U_{\mu(t)}(M(x))}{\partial \mu} \Psi. \quad (7)$$

One can then easily check that, for $\lambda = -\beta$, the corresponding equation and the initial condition $\Psi(x, \lambda, t=0) = \rho_0(x)$ is identically satisfied by

$$\Psi(x, -\beta, t) = \frac{e^{-\beta \mathcal{H}(x, t)}}{Z_0}. \quad (8)$$

Integrating this relation on x one obtains the usual form of the JE:

$$\langle e^{-\beta W} \rangle_t = \int dx \int dW e^{-\beta W} \Phi(x, W, t) = \frac{Z_{\mu(t)}}{Z_0} = \exp[-\beta(F_{\mu(t)} - F_0)] \quad (9)$$

Here Z_{μ} is the partition function corresponding to the hamiltonian $\mathcal{H}_0(x) + U_{\mu}(M(x))$, and $F_{\mu} = -k_B T \ln Z_{\mu}$ is the corresponding free energy. A more general relation is obtained if we multiply both sides of eq. (8) by $\delta(M - M(x))$ before integrating:

$$\langle \delta(M - M(x)) e^{-\beta W} \rangle_t = \int dx \delta(M - M(x)) \frac{e^{-\beta \mathcal{H}(x, t)}}{Z_0} = e^{-\beta[\mathcal{F}_0(M) + U_{\mu(t)}(M) - F_0]}. \quad (10)$$

Here $\mathcal{F}_0(M)$ is the free energy of a constrained ensemble, in which the value $M(x)$ is fixed at M :

$$\mathcal{F}_0(M) = -k_B T \ln \int dx \delta(M - M(x)) e^{-\beta \mathcal{H}_0(x)}. \quad (11)$$

Note that eq. (10) corresponds to eq. (21) in Crooks (ref. [4]), with the substitution $f(x) = \delta(M - M(x))$. It generalizes the expression by Hummer and Szabo (eq. 4, ref. [9]) to the

case in which the state of the system is represented by a collective coordinate. In this case the expression on the rhs of eq. (10) involves a free energy function rather than a microscopic hamiltonian.

By multiplying both sides of eq. (10) by $e^{\beta U_{\mu(t)}(M)}$, we obtain the basic identity of the histogram method:

$$e^{\beta U_{\mu(t)}(M)} \left\langle \delta(M - M(x)) e^{-\beta W} \right\rangle_t = e^{-\beta[\mathcal{F}_0(M) - F_0]}. \quad (12)$$

Equation (12) provides thus a method to evaluate the unperturbed free energy $\mathcal{F}_0(M)$ as long as one has a reliable estimate of the lhs of this equation. Note that that the quantity on the rhs of eq. (12) is a time independent quantity, and thus an improved estimate of $\mathcal{F}_0(M)$ can be obtained by sampling the rhs of eq. (12) at different time t along the manipulation process. The problem is that the quantities so obtained are not equally distributed, and so, their statistical treatment has to be performed conveniently, as described in the next section.

Equation (12) can be viewed as an extension of the JE (9). This last equation provides a method to evaluate the equilibrium free energy difference ΔF_t between the two thermodynamical states characterized by the external parameter values $\mu(t)$ and $\mu(0)$: one can in fact evaluate the quantity ΔF_t^* defined by the following equation

$$e^{-\beta \Delta F_t^*} = \frac{1}{N_{\text{traj}}} \sum_{i=1}^{N_{\text{traj}}} e^{-\beta W_t^i} \equiv \overline{e^{-\beta W_t}}. \quad (13)$$

The best estimate for ΔF_t will thus be given by $\Delta F_t \simeq \Delta F_t^*$.

3. Histogram method for the evaluation of the free energy landscape

Let us assume that we have n random variables x_i , $i = 1, \dots, n$, which are not identically distributed, but have the same average value $\langle x_i \rangle = X$. We wish to estimate X from a given sample $\{x_i\}$ of the x_i 's. Let us write the quantity x_i as a product of a random variable ξ_i and of a non-fluctuating factor a_i ,

$$x_i = \xi_i a_i. \quad (14)$$

One can obtain an estimate X_p of X from the set of data $\{x_i\}$ by a linear combination

$$X_p = \sum_{i=1}^n p_i x_i = \sum_{i=1}^n p_i \xi_i a_i, \quad (15)$$

where the coefficients p_i satisfy

$$p_i \geq 0; \quad \sum_{i=1}^n p_i = 1. \quad (16)$$

The best estimate of X is obtaining by minimizing the variance

$$\Delta X_p^2 = \langle X_p^2 \rangle - \langle X_p \rangle^2 \quad (17)$$

of the fluctuating quantity X_p , under the constraints (16). If one has

$$\sigma_i^2 = \langle \xi_i^2 \rangle - \langle \xi_i \rangle^2, \quad (18)$$

the variance of X_p is given by

$$\Delta X_p^2 = \sum_{i=1}^N p_i^2 a_i^2 \sigma_i^2. \quad (19)$$

By minimizing ΔX_p^2 , we thus obtain the following expression for the coefficients p_i :

$$p_i = \frac{\lambda}{a_i^2 \sigma_i^2}, \quad (20)$$

where λ is a Lagrange multiplier, which is fixed by the normalization condition of the coefficients p_i :

$$\lambda^{-1} = \sum_{i=1}^n \frac{1}{a_i^2 \sigma_i^2}. \quad (21)$$

The best estimate of X is thus given by

$$X_p^* = \lambda \sum_{i=1}^n \frac{\xi_i}{a_i \sigma_i^2}, \quad (22)$$

where λ is given by eq. (21).

As discussed above, we want to evaluate the rhs of equation (12) by sampling the experimentally accessible quantity which appears on the lhs of the same equation. We thus consider a number N_{traj} of repetitions of the experiment, and sample the corresponding trajectories at discrete times $t_j = j \delta t$. We also divide the interval of possible values of M into bins $B_\ell = [M_\ell, M_\ell + \delta M_\ell)$. Let us define the random variable

$$\begin{aligned} r(M_\ell, t_j) &= Z_0 e^{\beta U_{\mu(t_j)}(M_\ell)} \overline{\theta_\ell(M(t_j)) e^{-\beta W}} \\ &= Z_0 e^{\beta U_{\mu(t)}(M_\ell)} \frac{1}{N_{\text{traj}}} \sum_{k=1}^{N_{\text{traj}}} \theta_\ell(M_{t_j}^k) e^{-\beta W_{t_j}^k}, \end{aligned} \quad (23)$$

where the sum runs over N_{traj} independent repetitions of the manipulation process and $M_{t_j}^k$ is the value of the variable M along the k -th trajectory, at sampling time t_j . We have introduced the characteristic function $\theta_\ell(M)$ of the ℓ -th bin:

$$\theta_\ell(M) = \begin{cases} 1, & \text{if } M_\ell \leq M < M_\ell + \delta M_\ell; \\ 0, & \text{otherwise.} \end{cases} \quad (24)$$

Let

$$\rho(M_\ell, t_j) = \frac{1}{N_{\text{traj}}} \sum_{k=1}^{N_{\text{traj}}} \theta_\ell(M_{t_j}^k) e^{-\beta W_{t_j}^k} \quad (25)$$

define the stochastic part of the variable $r(M_\ell, t_j)$. We use $r(M_\ell, t_j)$ to estimate the quantity

$$\Delta R(M_\ell) = \exp[-\beta \mathcal{F}_0(M_\ell)] \delta M_\ell. \quad (26)$$

According to eq. (22) the best estimate for $\Delta R(M_\ell)$ is given by

$$\Delta R^*(M_\ell) = \lambda \sum_j \frac{\rho(M_\ell, t_j)}{a_{t_j}(M_\ell) \sigma_{t_j}^2(M_\ell)}, \quad (27)$$

where $a_t(M_\ell)$ is given by

$$a_{t_j}(M_\ell) = e^{\beta U_{\mu(t_j)}(M_\ell)}, \quad (28)$$

$\sigma_{t_j}^2(M_\ell)$ is given by

$$\begin{aligned} \sigma_{t_j}^2(M_\ell) &= \left\langle \rho^2(M_\ell, t_j) \right\rangle - \left\langle \rho(M_\ell, t_j) \right\rangle^2 \\ &= \frac{1}{N_{\text{traj}}^2} \sum_{k=1}^{N_{\text{traj}}} \left\langle \theta_\ell(M_{t_j}^k) e^{-2\beta W_{t_j}^k} \right\rangle - \left\langle \frac{1}{N_{\text{traj}}} \sum_{k=1}^{N_{\text{traj}}} \theta_\ell(M_{t_j}^k) e^{-\beta W_{t_j}^k} \right\rangle^2, \end{aligned} \quad (29)$$

and λ is defined by the normalization condition (21). In ref. [10], $\sigma_t^2(M)$ is taken to be

$$\sigma_t^2(M) = \frac{\overline{e^{-\beta W_t}}}{a_t(M)}. \quad (30)$$

Note that the quantity appearing on the numerator of eq. (30) does not necessarily satisfy the JE, since the mean is taken over a finite number of trajectories.

Note also that the rhs of eq. (13) is equal to the numerator of the fraction appearing on the rhs of eq. (30).

4. Evaluation of the free energy landscape of a mean field system

In the following we apply the histogram method, discussed in the previous section, to probe the free energy landscape of a known system, namely an Ising model in mean-field approximation, whose unperturbed free energy reads

$$\mathcal{F}_0(M) = -\frac{J}{2N} M^2 - TS(M), \quad (31)$$

where $S(M)$ is the usual entropy for an Ising paramagnet,

$$S(M) = -k_B \left[\left(\frac{N+M}{2} \right) \log \left(\frac{N+M}{2} \right) + \left(\frac{N-M}{2} \right) \log \left(\frac{N-M}{2} \right) \right]. \quad (32)$$

By using such a mean-field model, we can test how the different system's parameters affect the effectiveness of the histogram method to evaluate the free energy landscape. In particular we analyze the effect of changing the system size, the interaction parameter J_0 , the manipulation protocol, and the manipulation rate. The method described here can be easily generalized to systems characterized by any given free energy function, at least as long as the space of collective variables remains of small dimensionality.

The free energy landscape will be probed by applying an external magnetic field h , which is manipulated according to a given protocol $h(t)$. We assume that the system evolves according to Langevin dynamics, and thus the manipulation process can be simulated by numerically integrating the Langevin equation

$$\frac{\partial M}{\partial t} = -\beta v_0 \frac{\partial \mathcal{F}(M)}{\partial M} + \eta(t), \quad (33)$$

with

$$\langle \eta(t) \eta(t') \rangle = 2v_0 \delta(t - t'), \quad (34)$$

and where the total free energy $\mathcal{F}(M)$ is given by

$$\mathcal{F}(M) = \mathcal{F}_0(M) - hM \quad (35)$$

The Langevin equation (33) can be integrated using the Heun algorithm [14].

As discussed in the previous section, by sampling the quantity $\rho(M, t)$, eq. (25), we obtain the best estimate for $\mathcal{F}_0(M) = -k_B T \ln R^*(M)$, where $R^*(M)$ is defined by eq. (27). Here we adopt the expression (30) for $\sigma_t^2(M)$. Let us define the magnetization per spin $m = M/N$, N being the system size, then the quantity $f_0^*(m)$ defined as

$$f_0^*(m) = -\frac{k_B T}{N} \ln R^*(M), \quad (36)$$

will indicate in the following the estimated free energy per spin, for a given manipulation protocol. In order to quantify the quality of each estimate we divide the interval of values of m $[-1, 1]$ into N_m bins, and define the *distance* function

$$d \equiv \frac{1}{N_m} \sum_{i=0}^{N_m} [f_0(m_i) - f_0^*(m_i)]^2. \quad (37)$$

As we will see in the next subsections, the quality of the estimate of $\mathcal{F}_0(M)$ via eq. (36) is strictly connected to the the quality of the estimate of ΔF_t via eq. (13).

In the following, we fix the energy scale and the time scale by taking $\beta = 1$ and $\nu_0 = 1$.

4.1. Linear protocol

We first consider a linear protocol, which reads

$$h(t) = h_0 + \frac{h_1 - h_0}{t_f} t. \quad (38)$$

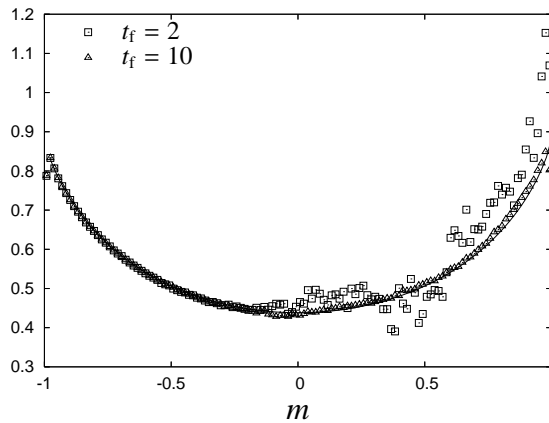


Figure 1. Comparison of the free energy landscape $f_0(m) = \mathcal{F}_0(M)/N$ (full line) with $J_0 = 0.5$, with the results of the simulations described in the text. The external magnetic field is varied according to the protocol (38) with $h_1 = -h_0 = 1$, and $t_f = 2, 10$. The system size is $N = 10$ and for each value of t_f , $N_{\text{traj}} = 10^4$ samples of the process are taken.

In figure 1, the expected free energy per spin $f_0(m) = \mathcal{F}_0(M)/N$, is plotted together with the estimated free energy $f_0^*(m)$, obtained with the method described above, for two values of

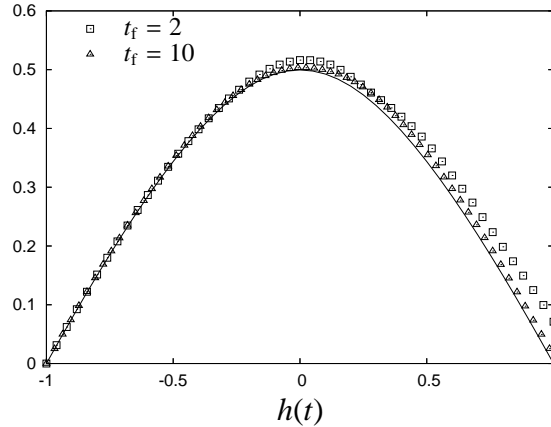


Figure 2. Comparison of the equilibrium free energy difference $\Delta f_t = f_{h(t)} - f_{h_0}$ as a function of $h(t)$ (full line), with the quantity F_t^*/N , as defined by eq. (13), obtained with the simulations described in the text. In these simulations the external magnetic field is varied according to the linear protocol (38) with $h_1 = -h_0 = 1$, and $t_f = 2, 10$. The mean field interaction parameter J_0 is taken to be $J_0 = 0.5$. The system size is $N = 10$ and for each value of t_f , $N_{\text{traj}} = 10^4$ samples of the process are taken.

the final time (inverse manipulation rate) t_f . This figure clearly shows that only the slowest process, with $t_f = 10$, gives a correct shape of the free energy $f_0(m)$ for any value of m . In figure 2, the quantity $\Delta F_t^*/N$, is plotted for the two manipulation rates, together with the equilibrium free energy difference $\Delta f_t = f_{h(t)} - f_{h_0}$, as functions of the external magnetic field $h(t)$. Comparison of fig. 1 with fig. 2 gives strong evidence that the effectiveness of the method here discussed for the reconstruction of the free energy landscape is strictly related to its effectiveness in evaluating the equilibrium free energy difference by using the JE. If the manipulation protocol is such that the free energy landscape is successfully reconstructed, then the estimate of the free energy difference, as given by eq. (13) is close to its expected value ΔF_t . On the other hand, one cannot expect $\mathcal{F}_0(M)$ to be reliably evaluated if the total free energy difference ΔF_t is poorly estimated. This conclusion is confirmed by changing the system parameters, e.g., by increasing the system size N . In figures 3 and 4 we plot the same quantities, namely $f_0^*(m)$ and $\Delta F_t^*/N$ for a larger system, with $N = 100$ spins. Also in this case the JE is effective in giving an accurate estimate of the free energy difference ΔF_t , if the protocol is slow enough for the free energy landscape to be reconstructed correctly.

4.2. Oscillatory protocol

In this subsection, the mean field system is manipulated according to the oscillatory protocol

$$h(t) = h_0 \sin(2\pi\nu t), \quad 0 \leq t \leq t_f. \quad (39)$$

We set $t_f = 2$, and take two values ($J_0 = 0.5, 1.1$) of the interaction parameter J_0 . The frequency ν is varied from $1/2$ up to 16. The function d , as defined by eq. (37) is plotted in figure 5 as a function of ν , for the two values of J_0 here considered.

In figure 6 the expected free energy per spin $f_0(m)$ is compared to the evaluated free energy for some of the values of ν here considered, for the $J_0 = 0.5$ case. Comparison of

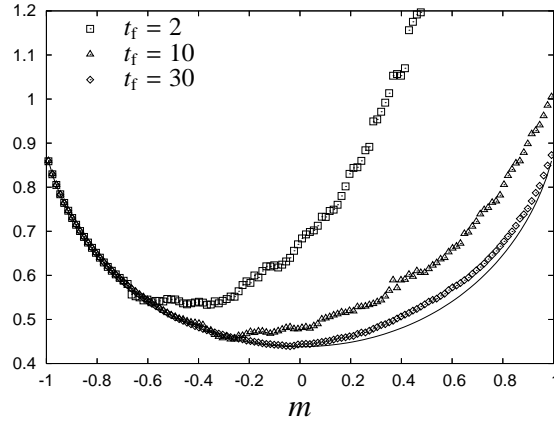


Figure 3. Comparison of the free energy landscape $f_0(m) = \mathcal{F}_0(M)/N$ (full line) with $J_0 = 0.5$, with the results of the simulations described in the text. The external magnetic field is varied according to the protocol (38) with $h_1 = -h_0 = 1$, and $t_f = 2, 10, 30$. The system size is $N = 100$ and for each value of t_f , $N_{\text{traj}} = 10^4$ samples of the process are taken.

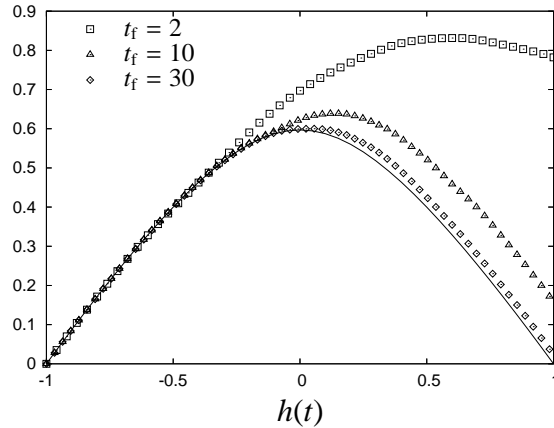


Figure 4. Comparison of the equilibrium free energy difference $\Delta f_t = f_{h(t)} - f_{h_0}$ as a function of $h(t)$ (full line), with the quantity F_t^*/N , as defined by eq. (13), obtained with the simulations described in the text. The mean field interaction parameter J_0 is taken to be $J_0 = 0.5$. In these simulations the external magnetic field is varied according to the linear protocol (38) with $h_1 = -h_0 = 1$, and $t_f = 2, 10, 30$. The system size is $N = 100$ and for each value of t_f , $N_{\text{traj}} = 10^4$ samples of the process are taken.

figures 5 and 6 clearly indicates that the optimal frequency for the reconstruction of the free energy landscape, with $J_0 = 0.5$, does not correspond to the smallest one but rather to $\nu \simeq 4$. The results discussed in subsection 4.1 suggest that the estimate of the free energy landscape is optimal for a manipulation protocol such that the estimate of the free energy difference Δf given by the JE is optimal. We thus consider the estimated free energy difference ΔF_t^* , as defined by eq.(13), for different values of the manipulation protocol frequency ν , and compare it to its expected value, see fig. 7(a). Since we are considering an oscillating protocol here, eq. (39), for a given value of h , there will be several estimates of Δf_t for different times t separated by the protocol period $1/\nu$. In figure 7(b), the mean value of F_t^*/N , obtained by averaging over these different contributions for a given value of h is plotted. As for the

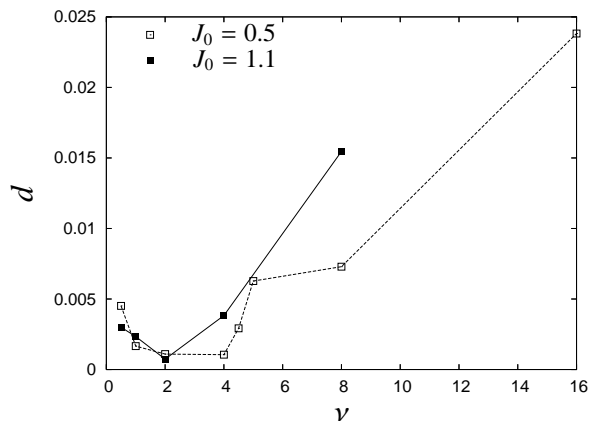


Figure 5. Distance function d , as defined by eq. (37), as a function of the frequency ν , for the oscillatory manipulation protocol (39). The size of the system is $N = 10$, and the number of trajectories is $N_{\text{traj}} = 10^4$. The line is a guide to the eye.

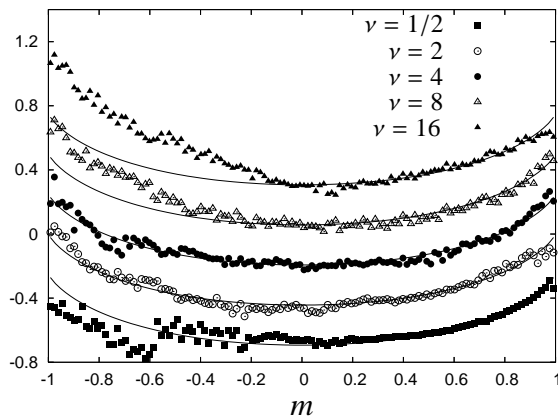


Figure 6. Plot of the estimated free energy landscape $f_0^*(m)$, obtained with the oscillatory protocol (39), for different values of the frequency ν , and with $J_0 = 0.5$. The sets of data are shifted to improve the clarity of the plot. The full lines correspond to the expected free energy landscape $f_0(m)$.

reconstruction of the energy landscape $f_0^*(m)$, the results shown in this last figure indicate that the optimal frequency value, for estimating the free energy difference ΔF_t is $\nu \simeq 4$.

We now consider the case $J_0 = 1.1$ and $t_f = 2$. In figure 8 the reconstructed free energy landscape $f^*(m)$ as given by eq. (36) is plotted, while in fig. 9 the estimated free energy difference ΔF_t^* , as defined by eq. (13), is plotted. The distance function d for the value of $J_0 = 1.1$ is plotted in fig. 5, as a function of the manipulation protocol frequency ν . Comparison of figures 5, 8 and 9 indicates that, for this value of J_0 , the optimal frequency is $\nu \simeq 2$, which is smaller than the value we find for the $J_0 = 0.5$ case.

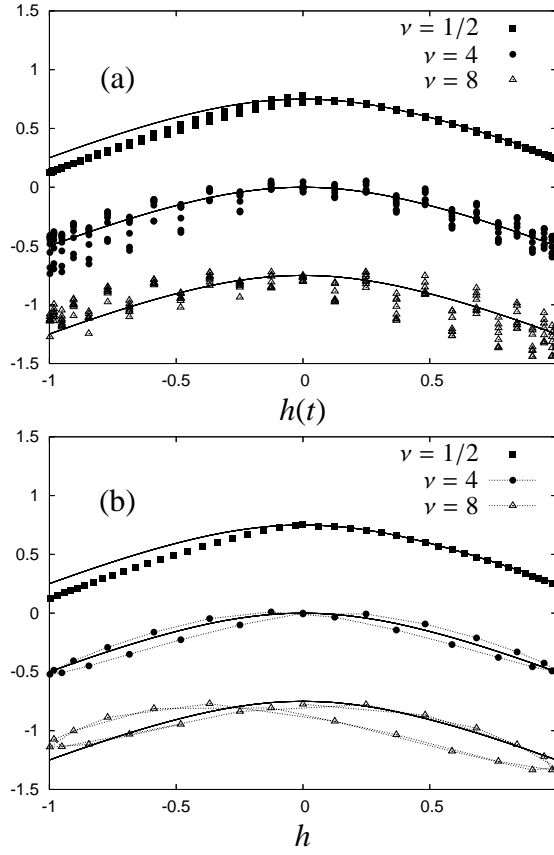


Figure 7. Comparison of the equilibrium free energy difference $\Delta f_t = f_{h(t)} - f_{h_0}$ as a function of $h(t)$ (full line), with the quantity F_t^*/N , as defined by eq. (13), obtained with the simulations described in the text. In these simulations the external magnetic field is varied according to the oscillatory protocol (39) with $h_0 = 1$, and $t_f = 2$. The mean field interaction parameter J_0 is taken to be $J_0 = 0.5$. The system size is $N = 10$ and $N_{\text{traj}} = 10^4$ samples of the process are taken. The sets of data are shifted to improve the clarity of the plot. Panel (b): mean value of F_t^*/N , obtained by averaging the contributions to this quantity for a given value of h , as plotted in panel (a). The dotted lines are guides to the eye.

5. Unzipping of a model homopolymer

In this section we consider a simple model of homopolymer subject to external forces. We aim thus to reconstruct the energy landscape of the polymer, as a function of its internal coordinate, namely its extension, via non-equilibrium manipulations.

The model polymer is made up of N identical beads which interact via a Lennard-Jones potential

$$U_{LJ} = \sum_{i=1, j < i}^N 4\epsilon \left[\left(\frac{\sigma}{r_{ij}} \right)^{12} - \left(\frac{\sigma}{r_{ij}} \right)^6 \right], \quad (40)$$

where r_{ij} is the distance between the i -th and the j -th monomers. Successive beads along the

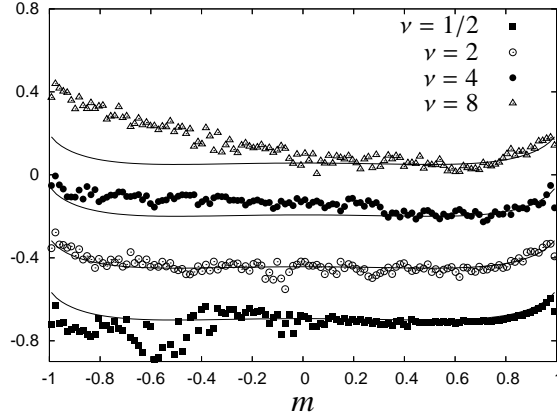


Figure 8. Plot of the estimated free energy landscape $f_0^*(m)$, obtained with the oscillatory protocol (39), for different values of the frequency ν and with $J_0 = 1.1$. The sets of data are shifted to improve the clarity of the plot. The full lines correspond to the expected free energy landscape $f_0(m)$.

polymer chain interact also via the harmonic potential

$$U_2 = \sum_{i=1}^{N-1} k(r_{i,i+1} - \sigma)^2. \quad (41)$$

We use here molecular dynamics simulations with Langevin noise: the equations of motion of the polymer beads thus read

$$m\ddot{\mathbf{r}}_i = \mathbf{F}(\mathbf{r}_i) - \gamma\dot{\mathbf{r}}_i + \boldsymbol{\eta}(t), \quad (42)$$

where m is the mass of the bead, $F(\mathbf{r}_i)$ is the force acting on the i -th bead due to the interaction with the remaining $N - 1$ beads, γ is the friction coefficient and $\boldsymbol{\eta}(t)$ is the random force satisfying

$$\langle \boldsymbol{\eta}(t) \rangle = 0; \quad (43)$$

$$\langle \eta_\alpha(t)\eta_\beta(t') \rangle = 2k_B T \gamma \delta(t - t'), \quad \alpha, \beta = x, y, z. \quad (44)$$

The values of the model polymer parameters are chosen following refs. [15, 16]: the Lennard-Jones energy ϵ and distance σ are taken to be $\epsilon = 1$ kcal/mol, $\sigma = 0.5$ nm, respectively, while the monomer mass is taken to be $m = 3 \cdot 10^{-25}$ kg. With this choice of the basic parameters one obtains a characteristic time $\tau \equiv \sqrt{m\sigma^2/\epsilon} \simeq 3.3$ ps. The strength of the harmonic bond potential (41) is taken to be $k = 5000 \epsilon/\sigma^2$, which corresponds to a more rigid bond than those considered in refs. [15, 16]. For the friction coefficient we take $\gamma = 15m/\tau$. The stochastic equations of motion for position and the velocity of the system's beads are solved using a modified leapfrog algorithm [17], with an integration time step $\delta t = 0.005\tau$, and where the temperature is fixed to $T = 300$ K .

In order to mimic the unfolding of the above described system with an external force exerted by an AFM cantilever, the polymer is manipulated according to the following procedure: the position of the first monomer of the chain is kept fixed, mimicking the trapping in the focus of an optical tweezers of infinite stiffness; at the starting time the last monomer of

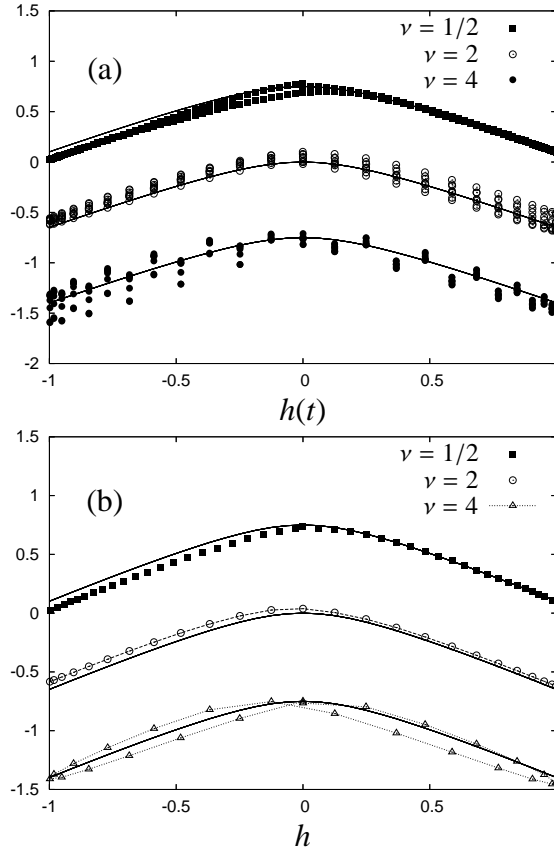


Figure 9. Comparison of the equilibrium free energy difference $\Delta f_t = f_{h(t)} - f_{h_0}$ as a function of $h(t)$ (full line), with the quantity F_t^*/N , as defined by eq. (13), obtained with the simulations described in the text. The mean field interaction parameter J_0 is taken to be $J_0 = 1.1$. In these simulations the external magnetic field is varied according to the oscillatory protocol (39) with $h_0 = 1$, and $t_f = 2$. The system size is $N = 10$ and $N_{\text{traj}} = 10^4$ samples of the process are taken. The sets of data are shifted to improve the clarity of the plot. Panel (b): mean value of F^*/N , obtained by averaging the contributions to this quantity for a given value of h , as plotted in panel (a). The dotted lines are guides to the eye.

the chain is “attached” to a pulling apparatus with a spring of elastic constant k (equal to the “molecular” stiffness appearing in eq. (41)), see figure 10. The external force is thus applied by moving the apparatus along a fixed direction with a protocol $z(t)$. Let ζ denote the distance of the N -th monomer from the plane containing the first monomer and perpendicular to the applied force direction, the external force reads thus $F_{\text{ext}} = k(z - \zeta)$.

As expected, we find that, in the absence of external force, the model polymer is in a globular state. Let ℓ be the end-to-end distance of the polymer, i.e., the distance between the last and the first monomer of the chain: $\ell = |\mathbf{r}_N - \mathbf{r}_1|$. We observe that in absence of external force, this quantity is $\ell = 2.31 \pm 0.08\sigma$. In order to define a typical collective time for the system, we measure the time needed to refold after a complete unfold, which we take to correspond to an end-to-end length $\ell = N\sigma$, we define this time t_F , which takes the value $t_F \approx 500\tau$ for the system size here considered. We also define the characteristic folding velocity $v_F \equiv N\sigma/t_F \approx 0.04\sigma/\tau$. These two quantities define the intrinsic time and velocity

scale of the polymer dynamics. In figure 11 the end-to-end length is plotted as a function of the time for a linear pulling protocol, with a constant velocity $\dot{z}(t) = 5 \cdot 10^{-5} \sigma/\tau$.

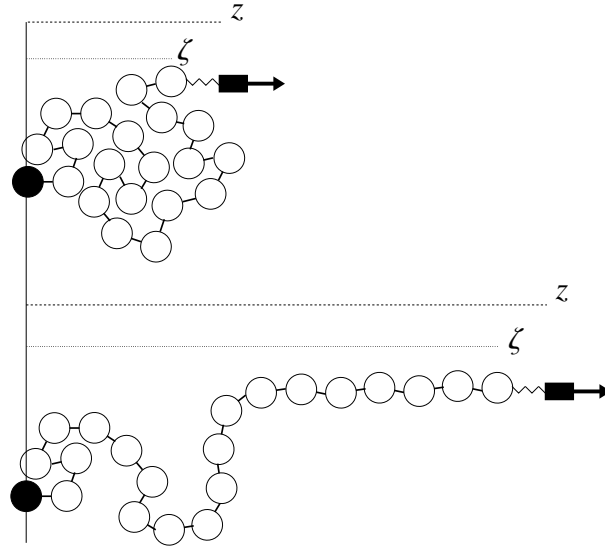


Figure 10. Cartoon of the mechanical unfolding of the model homopolymer. The coordinate z indicates the distance of the pulling apparatus from the reference plane, while the coordinate ζ indicates the distance of the N -th monomer from the reference plane, and represents the system collective coordinate.

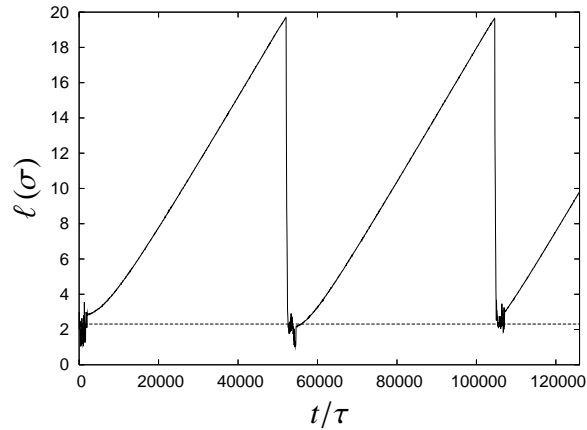


Figure 11. Polymer end-to-end length as a function of the time, for a linear pulling protocol, with velocity $\dot{z}(t) = 5 \cdot 10^{-5} \sigma/\tau$. The pulling apparatus is detached from the polymer after a fixed time $t = 50000\tau$ and then the system relaxes with no external force applied for a time interval $\Delta t = 2500\tau$. After that the external force is applied again.

We aim now to measure the system intrinsic free energy landscape as a function of the internal coordinate ζ using the method discussed in section 3. The work done on the polymer along a single trajectory reads

$$W = \int_0^{t_f} dt k [z(t) - \zeta(t)] \dot{z}(t). \quad (45)$$

Following equation (27), the best estimate for $\mathcal{F}_0(\zeta)$ is given by $\mathcal{F}_0(z) = -k_B T \ln R^*(\zeta)$ where $R^*(\zeta)$ is given by eq. (27), and $U_{\mu(t)}(\zeta) = \frac{k}{2} [z(t) - \zeta]^2$. As in the previous section we consider here both a linear protocol and an oscillatory protocol.

5.1. Linear protocol

In this section we consider the linear pulling protocol

$$z(t) = z_0 + vt, \quad (46)$$

where the constant z_0 is chosen to be slightly greater than the z -position of the N -th monomer at the beginning of each trajectory: $z_0 = \zeta(t = 0) + \sigma/100$. Here we consider three values of the pulling velocity, $v = 5 \times 10^{-4}, 5 \times 10^{-3}, 5 \times 10^{-2} \sigma/\tau$. For each velocity, the duration time of the manipulation t_f is chosen in such a way that the stroke of the pulling apparatus is $\Delta z = 25\sigma$, and the polymer is fully unfolded. This corresponds to a time interval of $t_f = 500000, 50000, 5000\tau$ for the the three protocols, respectively. For the slowest velocity we take 50 repetitions of the pulling process, for the intermediate velocity we take 500 repetitions, while for the fastest velocity we take 1000 repetitions of the pulling process. After each pulling process, the polymer evolves at zero force for a time interval of $5t_f = 2500\tau$, mimicking the detachment of the pulling apparatus and the refolding of the polymer.

In fig. 12 we compare the free energy landscape $\mathcal{F}_0^*(\zeta)$ obtained from the three pulling velocities, by using the histogram method discussed in section 3. Differently from the Ising model, in this case, we do not know the expected free energy function. However, in order to perform a consistency check one can note that the free energy difference $\Delta F_{z(t)} = F(z(t)) - F(z(0))$, which is function of the pulling apparatus coordinate $z(t)$, and the free energy landscape $\mathcal{F}_0(\zeta)$ are related via

$$\Delta F_{z(t)} = -k_B T \ln \left[\int d\zeta e^{-\beta[\mathcal{F}_0(\zeta) + \frac{k}{2}(z(t) - \zeta)^2]} \right] + \text{const.} \quad (47)$$

Our best estimate for $\Delta F_{z(t)}$ is obtained by averaging $\exp(-\beta W_t)$ over the repetitions of the pulling process, as given by eq.(13). In the limit of $\dot{z} \rightarrow 0$, we expect this estimate to be exact. In figure 13, we compare the free energy difference obtained with direct measuring, eq. (13), and that obtained using eq. (47), for the fastest pulling velocity here used. Inspection of this figure suggests that the agreement between the two estimates of $\Delta F_{z(t)}$ is rather good for this value of the velocity. The agreement is also good for the two other values of the pulling velocity (data not shown).

5.2. Oscillatory protocol

Here, the polymer is manipulated by varying the pulling apparatus position according to the protocol

$$z(t) = \frac{z_{\max}}{2} [1 - \cos(2\pi vt)] + z_0, \quad (48)$$

where the constant z_0 is chosen to be slightly greater than the z -position of the N -th monomer at the beginning of each trajectory: $z_0 = \zeta(t = 0) + \sigma/100$. The value of z_{\max} is taken to

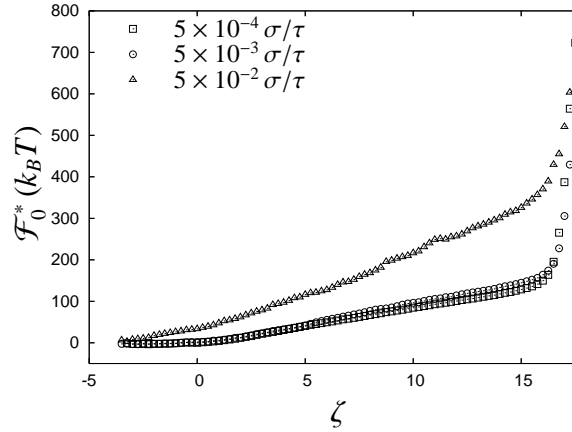


Figure 12. Reconstructed free energy landscape \mathcal{F}_0^* as a function of the polymer internal coordinate ζ , obtained with the linear protocol (46), for the three pulling velocities here considered. The line, in the case of the faster velocity, is a guide to the eye.

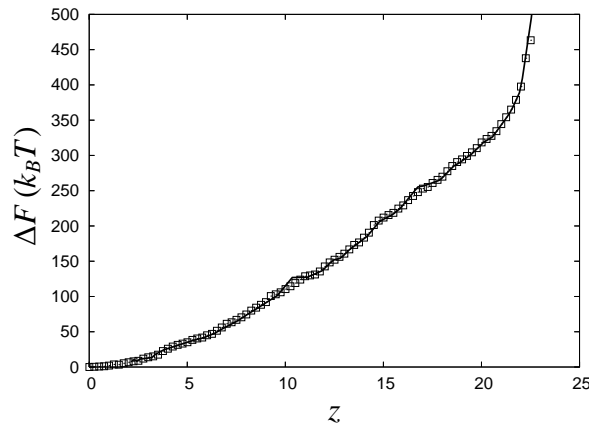


Figure 13. Free energy difference ΔF as a function of the pulling apparatus coordinate z , for the linear protocol (46), with the largest pulling velocity here used $\dot{z} = 5 \times 10^{-2} \sigma/\tau$. Squares: free energy difference ΔF obtained using the JE (13). Full line: free energy difference ΔF as given by eq. (47).

be $z_{\max} = (N + 4)\sigma$, in such a way that the polymer is fully unfolded near the maximum of the function (48). Three values of the frequency $\nu = 5 \times 10^{-6}, 5 \times 10^{-5}, 5 \times 10^{-4} \tau^{-1}$ are considered here. These values have to be compared with the system characteristic frequency ν_F as estimated in section 5, $\nu_F = 1/t_F \approx 2 \times 10^{-3} \tau^{-1}$. Let us define the effective velocity

$$v_{\text{eff}} \equiv \left(\nu \int_0^{1/\nu} dt \dot{z}^2(t) \right)^{\frac{1}{2}} = \frac{z_{\max} \pi \nu}{\sqrt{2}}, \quad (49)$$

the three frequencies here considered correspond to the values of the effective velocity $v_{\text{eff}} \approx 2.66 \times 10^{-4}, 2.66 \times 10^{-3}, 2.66 \times 10^{-2} \sigma/\tau$ respectively. These velocities have to be compared with the characteristic folding velocity of the polymer as estimated in section 5, $\nu_F = 0.04 \sigma/\tau$. We adopt two different approaches to manipulate the polymer: in the first case the pulling apparatus is always attached to the polymer during the whole manipulation time t_f , fig. 14(a), while in the second case the pulling apparatus is detached after one and

half period $1/\nu$ of the protocol, the system equilibrates at zero force for a time interval of $5t_F$, and then the force is applied again, see figure 14(b). In the case where the pulling

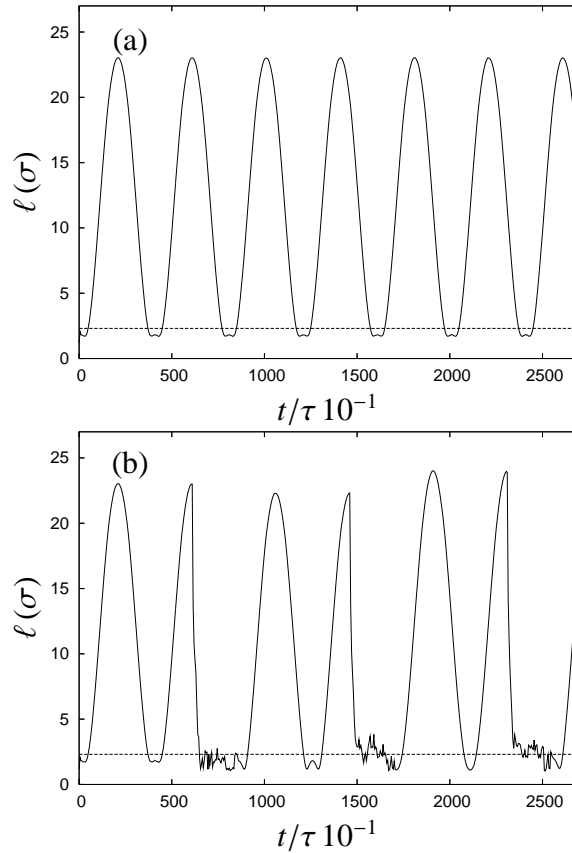


Figure 14. Polymer end-to-end length as a function of the time, for the periodic manipulation protocol (48), with frequency $\nu = 5 \times 10^{-4} \tau^{-1}$. The dotted line represents the mean value of the polymer end-to-end length in absence of external force. Panel (a): the pulling apparatus stays in contact with the polymer during the whole manipulation process. Panel (b): the pulling apparatus is detached from the polymer after a fixed time $1.5/\nu\tau$ and then the system relaxes with no external force applied for a time interval $\Delta t = 2500\tau$. After that the external force is applied again.

apparatus is attached during the whole manipulation process, we take a total manipulation time $t_f = 10^7 \tau$. In the case where the pulling apparatus is detached after one and half period, we consider 50 trajectories for $\nu = 5 \times 10^{-6}$, 500 trajectories for $\nu = 5 \times 10^{-5}$, and 1000 trajectories for $\nu = 5 \times 10^{-4}$. The results for the reconstructed free energy landscape with these two manipulation strategies are plotted in fig. 15. Inspection of figure 15(a) clearly puts in evidence that the “always attached” protocol (fig. 14(a)) gives a good estimates for the free energy landscape only for the smallest frequency here considered $\nu = 5 \times 10^{-6} \tau^{-1}$, which corresponds to an effective velocity $v_{\text{eff}} = 2.66 \times 10^{-4} \sigma/\tau$; while for the two other frequencies the reconstructed free energy landscape is completely wrong. This can be easily understood by looking at fig. 16: after a complete unfolding, if the molecule is pulled leftwards too fast, it cannot achieve the native globular state, and so the internal coordinate ζ , will be no longer a “good” collective coordinate to describe the system state. Note that the periodic protocol

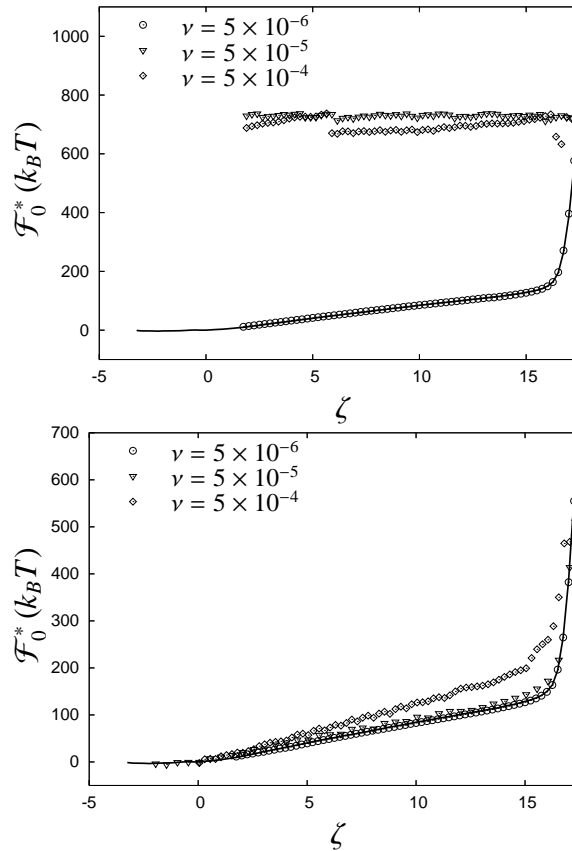


Figure 15. Reconstructed free energy landscape \mathcal{F}_0^* as a function of the polymer internal coordinate ζ , obtained with the oscillatory protocol (48) for the three frequency ν here considered. The full line is the “reference” free energy landscape \mathcal{F}_0 obtained with the linear protocol (46) with the smallest velocity $\nu = 5 \times 10^{-4} \sigma/\tau$. Upper panel: the free energy landscape \mathcal{F}_0 is reconstructed using the “always-attached” manipulation protocol, fig. 14(a). Lower panel: the free energy landscape \mathcal{F}_0 is reconstructed by periodically detaching the pulling apparatus, fig. 14(b).

proves unsuccessful to recover the energy landscape for frequency well below the system characteristic frequency ν_F .

In the case of the second manipulation strategy, the reconstructed energy landscape, fig. 15(b), agrees with that obtained with the linear protocol for the two smallest frequency here considered. On the contrary, the reconstructed energy landscape obtained with the largest frequency $\nu = 5 \times 10^{-4}$ is clearly inaccurate.

It is worth to note that for our purpose, i.e. the reconstruction of the free energy landscape, the “pulsed” protocol, represented in figure 14(b) is to all extent equivalent to the linear protocol (46).

6. Discussion

In the present work we have combined the extended form of the JE, eq. (12), and the histogram method to reconstruct the free energy landscape of two simple systems driven out

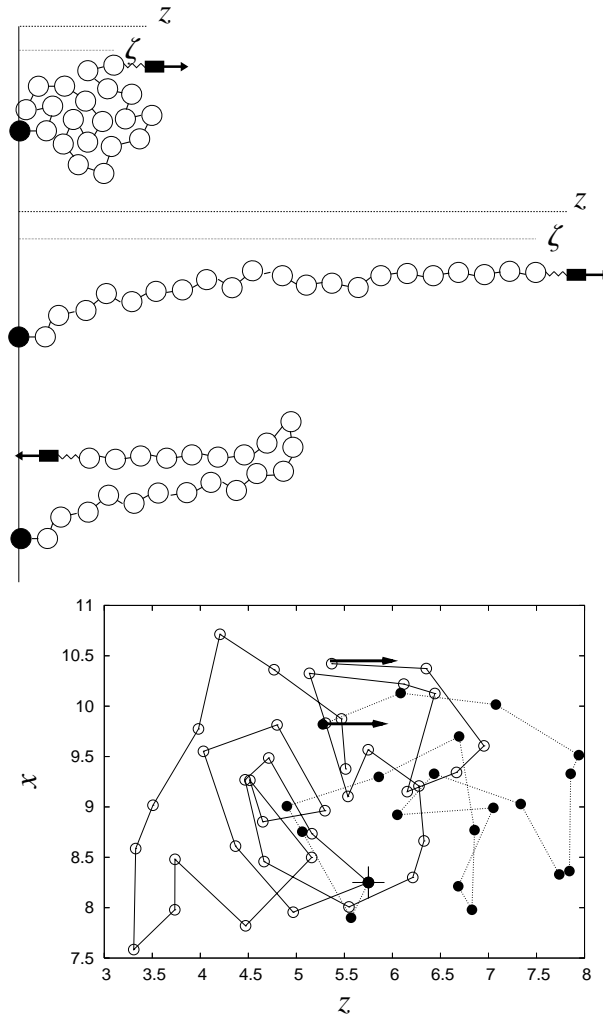


Figure 16. Upper panel: Cartoon of the polymer manipulation. The polymer is manipulated with the oscillatory protocol (48). If the polymer is manipulated too fast, it cannot attain the globular native state after one manipulation cycle. Lower panel: snapshots of the polymer configuration, at two different times of a simulation run with $\nu = 5 \times 10^{-4} \tau^{-1}$, projected onto the $z - x$ plane. Empty circles- full line: Configuration at $t = 0$, i.e. the system is at thermodynamical equilibrium with no external force applied. Full circles- dotted line: configuration of the system after one manipulation period. The cross indicates the fixed monomer, the arrows indicate the monomers to which the force is applied.

of equilibrium by manipulation of an external parameter.

In the case of the Ising model in mean field approximation, the external magnetic field is manipulated both with a linear and with a periodic protocol. In both cases, for a sufficiently gentle protocol, the system free energy landscape is successfully evaluated. It is worth to note that, for the periodic protocol, the optimal frequency for the reconstruction of the landscape is somewhat larger than the smallest frequency here considered. This indicates the existence of a typical system frequency, which optimizes the estimate given by the histogram method, as already found in [10]. However, we point out that this typical frequency is of the order of the frequency governing the system dynamics, which has been taken equal to one in the

present work. This means that the manipulation has to be performed on time scales similar to the system characteristic time scale, in order for the free energy evaluation method here discussed to be successful. Faster manipulations give unreliable estimates of the free energy function. In the case of the linear protocol we also consider the effect of the system size on the effectiveness of the histogram method. As discussed in refs. [12, 13], changing the system size N corresponds to change the system energy scale. There, we showed that one can obtain a good estimate of the free energy difference, via the JE, only for small system sizes (small energy scales). Similarly, the results of the present works indicate that the histogram method is effective for small system sizes. This conclusion widens the results of refs. [9, 10] on the histogram method, since in those references the effect of the energy scale was not considered.

The second system here considered is a simple model of homopolymer, which is unzipped by applying an external force to one of its free ends. Also in this case the external force is varied both with a linear and with a periodic protocol. The results of this simulated experiment have to be considered more carefully, with respect to the case of the Ising model, since we do not know the exact shape of the polymer free energy landscape. We take as our best estimate of this landscape the one provided by the linear protocol with the smallest velocity. We find that the periodic force gives unreliable estimates of the free energy as a function of the polymer elongation, even for frequencies much smaller than the system characteristic frequency. This is at variance with the conclusions of ref. [10], where the periodic loading was found to be the optimal one for the evaluation of the free energy landscape of a model polymer. The reason for this discrepancy resides in the fact that our model polymer takes also into account the three-dimensional structure of the system, and when a periodic force is applied, the elongation coordinate is no longer a “good” collective coordinate, and fails to catch the connection between the system macroscopic state and its microscopic state, as depicted in fig. 16. In fact, the system has no time to recover its initial globular state, and keeps memory of previous trajectories at each manipulation cycle.

Our results suggest thus that in the realization of a real experimental set-up, if one wants to exploit the histogram method to evaluate the free energy landscape of a polymer, some care has to be taken with the choice of the manipulation protocol. The linear protocol, or the “pulsed” sinusoidal protocol, appear to be the best choices to this purpose. This is closely related to the original proposition of the JE, which states that the equality holds *if* the system is in thermodynamical equilibrium at the beginning of the manipulation.

Finally, we have found that the polymer elongation is not a good state variable to describe the system when the manipulation occurs on too short times, since the system is not able to reach a quasi-equilibrium state defined by its instantaneous value. In this case, the concept of a free-energy landscape depending on this coordinate is ill-defined.

Acknowledgments

This research was partially supported by MIUR-PRIN 2004.

References

- [1] M. Carrion-Vasquez *et al*, PNAS **96**, 3694 (1999); J. Liphardt, B. Onoa, S. B. Smith, I. Tinoco, and C. Bustamante, Science **292**, 733 (2001); F. Ritort, C. Bustamante, and I. Tinoco Jr., Proc. Natl. Acad. Sci. USA **99**, 13544 (2002); B. Onoa, S. Dumont, J. Liphardt, S. B. Smith, I. Tinoco, and C. Bustamante, Science **299**, 1892 (2003).
- [2] C. Jarzynski, Phys. Rev. Lett. **78**, 2690 (1997); C. Jarzynski, Phys. Rev. E **56**, 5018 (1997).
- [3] G. E. Crooks, J. Stat. Phys. **90** 1481 (1998).
- [4] G. E. Crooks, Phys. Rev. E **61** 2361 (1999).
- [5] J. Gore, F. Ritort, and C. Bustamante, Proc. Natl. Acad. Sci. USA **100**, 12564 (2003).
- [6] F. Ritort, J. Stat. Mech.: Theory Exp. **10**, P10016 2004 .
- [7] C. H. Bennett, *J. Comp. Phys.*, **22**, 245 (1976).
- [8] A. M. Ferrenberg and R. H. Swendsen, *Phys. Rev. Lett.*, **63**, 1195 (1989).
- [9] G. Hummer and A. Szabo, Proc. Natl. Acad. Sci. USA **98**, 3658 (2001).
- [10] Braun, A. Hanke, and U. Seifert, *Phys. Rev. Lett.*, **93**, 158105 (2004).
- [11] T. Speck and U. Seifert, Phys. Rev. E, **70**, 066112 (2004).
- [12] A. Imparato and L. Peliti, *Europhys. Lett.*, **70**, 740-746 (2005).
- [13] A. Imparato and L. Peliti, *Phys. Rev. E*, **72**, 046114 (2005).
- [14] See, e.g., A. Greiner, W. Strittmatter, and J. Honerkamp, J. Stat. Phys. **51**, 95 (1988) and R. Mannella, Int. J. Mod. Phys. C **13**, 1177 (2002).
- [15] T. Veitshans, D. Klimov, and D. Thirumalai, *Folding Des.* **2**, 1 (1997).
- [16] T.X. Hoang and M. Cieplak, *J. Chem. Phys.* **112**, 6851 (2000).
- [17] R. Mannella, *Phys. Rev. E* **69**, 041107 (2004).